

16 -

CT

:

1

2

3

4

: 16 - MDCT (Multidetector CT arthrography, CTA)
: CTA 45
. CTA ,

CTA , ,
: SLAP ($n=33$) Bankart ($n=6$) SLAP
type I 9 , type II 23 , type III 1
9 , 1 . type I 24 SLAP CTA
83%, 100%, 91% . CTA 90%,
100%, 98% , 100%, 94%,
96% , 29%, 100%, 89% .
: 16 - MDCT
MRI .

가

(1 - 4).

가

2004 5

2005 12

CTA

112

45

CT (Multidetector - row CT, MDCT)

가

. CTA

18

가

51 (19 - 78) ,

가

(5).

가 30 ,

가 15 ,

32 ,

13 .

16 -

(Omnipaque 350, 35%

CT (CT arthrography, CTA)

isohexol, Amersham Health, Cork, Ireland) 7 mL,

13 mL Epinephrine 0.3 mL

16 -

CT

5 - 17 mL (12 mL)

21 gauge

CTA

Jacobson (6)

10

16 -

MDCT (Somatom sensation 16, Siemens, Erlangen, Germany)

. 16 × 0.75 mm collimation, 9 mm

(pitch, 4.5), 0.5 , 120 kV,

150 mA .

2005

2006 9 11

2007 2 2

CTA 18 (1 - 150)
 가 . 가 ,
 45 33
 SLAP type I 9 (27%), type II가
 23 (70%), type III가 1 (3%) (Fig. 2) , 6
 Bankart (Table 1). type I SLAP
 9 CTA
 type I SLAP
 24 SLAP
 46 (19 - 75) , 가 19 , 가 5 ,
 16 , 8 type II III
 SLAP 40 50 5 가
 , 20 60 4 , 30 3 , 70 2 , 10
 1 . 23 type II SLAP 4
 CTA . type II SLAP

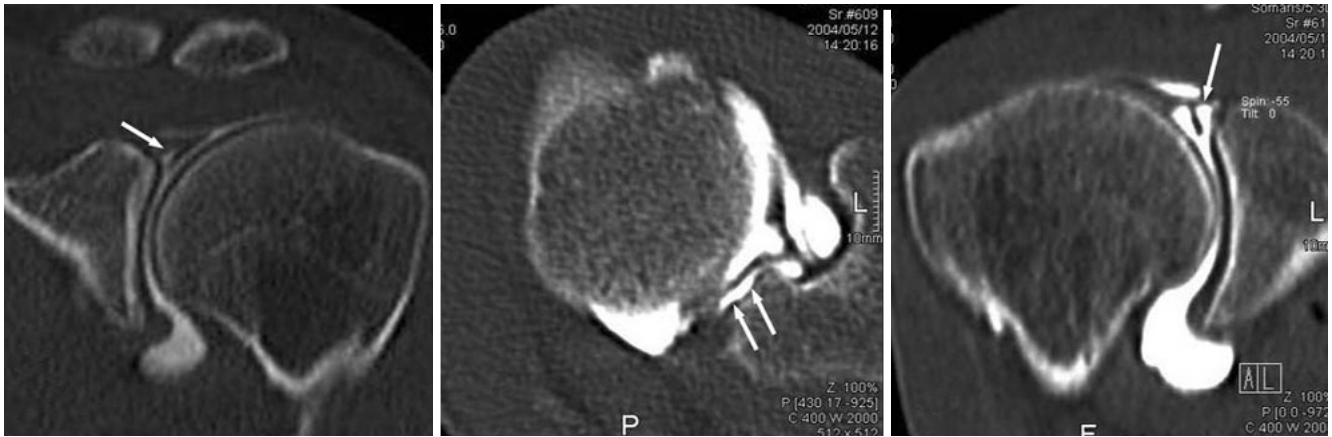


Fig. 1. Type II SLAP lesion.
A. Coronal reformatted image shows contrast material between the superior labrum and the glenoid (arrow), which is oriented in a lateral direction away from the glenoid rim.
B. Axial CT arthrogram shows contrast material deposits (arrows) posterior to the biceps tendon insertion.
C. Coronal reformatted image shows wide separation (arrow) between the superior labrum and the glenoid.

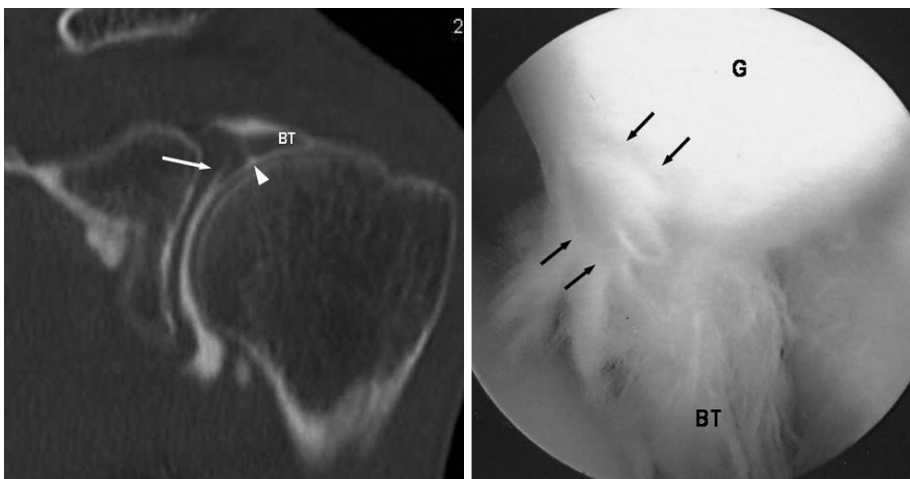


Fig. 2. Type III SLAP lesion.
A. Coronal reformatted image shows contrast material interposed between the labrum and the glenoid (arrow) as well as between the labrum and the biceps tendon (BT) (arrowhead).
B. Arthroscopic view obtained from a posterior portal confirms the presence of a type III SLAP lesion (arrows).

CTA 83% (20/24), 31, 21
 100% (21/21), 91% (41/45), 6 Bankart 9, 1
 100% (6/6), 97% (38/39), 7, 1
 98% (44/45) 45 22 3). 22 62 (50 - 75), 가 11, 가 11, 15, 7
 CTA 90% (28/31), 100% (104/104), 98% (132/135), 94% (29/31), 96% (43/45), 100% (14/14), 29% (2/7), 100% (38/38), 89% (40/45) (Table 3).
 CTA 3, 3



Fig. 3. Large full-thickness supraspinatus tear. Coronal reformatted image shows contrast material in the subacromial/subdeltoid bursa (arrowheads). The tendon margin (arrow) is retracted from the greater tuberosity.

가
 ,
 (3, 10).
 가
 가
 가
 16 - CT (multiplanar)

Table 1. Correlation Between Findings at CT Arthrography and Arthroscopy for Superior Labral Anteroposterior(SLAP) Lesions

CTA	Arthroscopy				
	N (n=12)	I (n=9)	II (n=23)	III (n=1)	IV (n=0)
N (n=25)	12	9	4	0	0
I (n=0)	0	0	0	0	0
II (n=17)	0	0	17	0	0
III (n=3)	0	0	2	1	0
IV (n=0)	0	0	0	0	0

I, II, III, IV; type of SLAP lesion, N ; Normal

Table 2. Correlation Between Findings at CT Arthrography and Arthroscopy for Rotator Cuff Tears

CT Arthrography	N (n=104)	Arthroscopy				
		SSP		ISP		SSC
		FT (n=14)	PT (n=7)	FT (n=7)	PT (n=2)	FT (n=1)
N (n=107)	104	0	3*	0	0	0
SSP FT (n=16)	0	14	2	0	0	0
PT (n=2)	0	0	2	0	0	0
ISP FT (n=6)	0	0	0	6	0	0
PT (n=3)	0	0	0	1	2	0
SSC FT (n=1)	0	0	0	0	0	1

The numbers(n=135) are those of total rotator cuffs excluding teres minor tendon of 45 patients.

FT; Full-thickness tear, PT; Partial-thickness tear, N; Normal, SSP; Supraspinatus tendon, ISP; Infraspinatus tendon, SSC; Subscapularis tendon, *; Tears on the bursal surface

reformation)

가 CTA 가
(11, 12).
CTA

Candnani (4) CTA 73%
96%
MDCT
Choi (13) Bitzer (14)
96%
Choi 80%, 88%, Bitzer
76%, 92%
type II SLAP CTA가
95%
CTA type II SLAP
83%, 100%, 91%
type I SLAP 9
CTA
type II SLAP 2
1

Table 3. Efficacy of CT Arthrography in the Diagnosis of Rotator Cuff Tears

	Total (SSP + ISP + SSC)	FT (SSP)	PT (SSP)
Sensitivity (%)	28/31 (90)	14/14 (100)	2/7 (29)
Specificity (%)	104/104 (100)	29/31 (94)	38/38 (100)
Accuracy (%)	132/135 (98)	43/45 (96)	40/45 (89)

FT; Full-thickness tear, PT; Partial-thickness tear, SSP; Supraspinatus tendon, ISP; Infraspinatus tendon, SSC; Subscapularis tendon

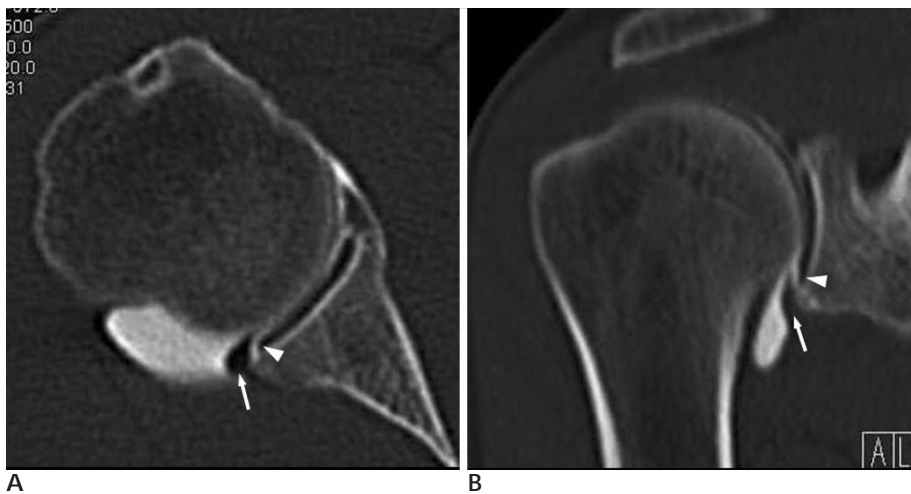


Fig. 4. Normal gap of the posteroinferior labrum. (A) Axial and (B) coronal reformatted images show contrast filled smooth gap between the posteroinferior articular cartilage (arrowhead) and labroligamentous complex (arrow).



Fig. 5. Posterior joint capsular rupture. (A) Axial, (B) sagittal and (C) coronal reformatted images show focal discontinuity at the posterior joint capsule (arrow) with extravasation of the contrast material around the teres minor muscle (arrowheads).

type I SLAP

CTA 가 type 가

II SLAP CTA 가

(10), 16 - CT 가

Charousset (15) 259 CTA 99%, 100%, 97%, 100%

100%, 가 90%, 100%, 98%, 94%, 96%, 29%, 100%, 89%

(Superior sublabral sulcus), Buford 가 (1).

CTA Bankart 1, 2

CTA (Fig. 4). 가

Bankart 가 (Fig. 5). 가

CTA 가 가

가 가

가 16 - CTA

1. De Maeseneer MD, Van Roy F, Lenchik L, Shahabpour M, Jacobson F, Ryu KN, et al. CT and MR arthrography of the normal and pathologic anterosuperior labrum and labral-bicipital complex. *Radiographics* 2000;20:S67-S81
2. McCarthy C. Glenohumeral instability. *Imaging* 2003;15:174-179
3. Beltran J, Rosenberg ZS, Chandnani VP, Cuomo F, Beltran S, Rokito A. Glenohumeral instability: evaluation with MR arthrography. *Radiographics* 1997;17:657-673
4. Chandnani VP, Yeager TD, DeBerardino T, Christensen K, Gagliardi JA, Heitz DR, et al. Glenoid labral tears: prospective evaluation with MR imaging, MR arthrography, and CT arthrography. *AJR Am J Roentgenol* 1993;161:1229-1235
5. Blum A, Coudane H, Mole D. Gleno-humeral instabilities. *Eur Radiol* 2000;10:63-82
6. Jacobson JA, Lin J, Jamadar DA, Hayes CW. Aids to successful shoulder arthrography performed with a fluoroscopically guided anterior approach. *Radiographics* 2003;23:373-379
7. Bencardino JT, Beltran J, Rosenberg ZS, Rokito A, Schmahmann S, Mota J, et al. Superior labrum anterior-posterior lesions: diagnosis with MR arthrography of the shoulder. *Radiology* 2000;214:267-271
8. Smith DK, Chopp TM, Aufdemorte TB, Witkowski EG, Jones RC. Sublabral recess of the superior glenoid labrum: study of cadavers with conventional nonenhanced MR imaging, MR arthrography, anatomic dissection, and limited histologic examination. *Radiology* 1996;201:251-256
9. Snyder SJ, Karzel RP, Del Pizzo W, Ferkel RD, Friedman MJ. SLAP lesions of the shoulder. *Arthroscopy* 1990;6:274-279
10. Ostlere S. Imaging the shoulder. *Imaging* 2003;15:162-173
11. Vande Berg BC, Lecouvet FE, Poilvache P, Maldague B, Malghem J. Spiral CT arthrography of the knee: technique and value in the assessment of internal derangement of the knee. *Eur Radiol* 2002;12:1800-1810
12. Waldt S, Bruegel M, Ganter K, Kuhn V, Link TM, Rummeny EJ, et al. Comparison of multislice CT arthrography and MR arthrography for the detection of articular cartilage lesions of the elbow. *Eur Radiol* 2005;15:784-791
13. Choi JA, Lee IS, Oh JH, Lee JW, Choi JY, Hong SH, et al. 16 slice multidetector CT arthrography in the evaluation of labral and rotator cuff lesions of the shoulder: a preliminary study with comparison with direct MR arthrography and arthroscopic correlation. *ISS 32nd Annual Refresher Course Sep 28-Oct 1: Raffles City Convention Centre: Singapore; 2005*
14. Bitzer M, Nasko M, Krackhardt T, Schick F, Schober W, Wiskirchen J, et al. Direct CT-arthrography versus direct MR-arthrography in chronic shoulder instability: comparison of modalities after the introduction of multidetector-CT technology. *Rofo* 2004;176:1770-1775
15. Charousset C, Bellaiche L, Duranthon LD, Grimberg J. Accuracy of CT arthrography in the assessment of tears of the rotator cuff. *J Bone Joint Surg Br* 2005;87:824-828

16-Slice MDCT Arthrography of the Shoulder: Accuracy for Detection of Glenoid Labral and Rotator Cuff Tears¹

Gang-Deuk Kim, M.D., Sung-Ah Lee, M.D.², Huoung-Jun Kim, M.D.³, Hye-Won Kim, M.D.,
Jung-Taek Oh, M.D.⁴, Seon-kwan Juhng, M.D.

¹Department of Diagnostic Radiology, ²Orthopaedic Surgery, ³General Surgery, Wonkwang University Hospital

²Department of Diagnostic Radiology of Seoul Medical Center

Purpose: We wanted to determine the diagnostic accuracy of 16-slice MDCT arthrography (CTA) for glenoid labral and rotator cuff tears of the shoulder.

Materials and Methods: We enrolled forty-five patients who underwent arthroscopy after CTA for pain or instability of the shoulder joint. The CTA images were analyzed for the existence, sites and types of glenoid labral tears and the presence and severity of rotator cuff tears. We determined the sensitivity, specificity and accuracy of CTA for detecting glenoid labral and rotator cuff tears on the basis of the arthroscopy findings.

Results: At arthroscopy, there were 33 SLAP lesions (9 type I, 23 type II and 1 type III), 6 Bankart lesions and 31 rotator cuff lesions (21 supraspinatus, 9 infraspinatus and 1 subscapularis). On CTA, the sensitivity, specificity and accuracy for detecting 24 SLAP lesions, excluding the type I lesions, were 83%, 100% and 91%, the total rotator cuff tears were 90%, 100% and 98%, the full thickness supraspinatus tendon tears were 100%, 94% and 96%, and the partial thickness supraspinatus tendon tears were 29%, 100% and 89%, respectively.

Conclusion: 16-slice MDCT arthrography has high accuracy for the diagnosis of abnormality of the glenoid labrum or rotator cuff tears and it can be a useful alternative to MRI or US.

Index words : Shoulder, CT

Shoulder, arthrography

Shoulder, abnormalities

Shoulder, injuries

Address reprint requests to : Seon-kwan Juhng, M.D., Department of Diagnostic Radiology, Wonkwang University Hospital,
344-2 Shinyong-dong, Iksan 570-711, Korea.
Tel. 82-63-850-1514 Fax. 82-63-851-4749 E-mail: juhngsk@wonkwang.ac.kr